FATIGUE CRACK GROWTH IN HARD STEELS

R A Smith*

Fracture and fatigue crack growth data for a medium hardness tool steel and a high hardness bearing steel are compared with data in the literature for both similar and softer materials. For the high hardness steel, stable crack growth is confined to a narrow band of ΔK values, and rates are considerably in excess of those for softer steels because of increased static modes of failure. An unsuccessful attempt was made to generate Mode II in the bearing steel.

INTRODUCTION

Fracture mechanics fatigue crack growth data has been generated for many metallic materials. The data is usually in the form of growth rate (da/dN) as a function of applied stress intensity factor range (ΔK), and is easily retrievable from the literature, e.g. the Compendia produced by Hudson and Seward, (1) and (2). However, little of this kind of data exists for hard steels. This may be because of the experimental difficulties associated with the production of such data, or because of the apparent lack of practical significance of fatigue crack growth in hard steels. This paper reports tests conducted on two different steels, an H13 tool steel and an SAE 52100 martensitic hardened steel, compares the data produced with the existing data for both hard and structural steel and finally discusses the practical significance of crack growth in hard steels.

*Cambridge University Engineering Department, Trumpington Street, Cambridge CB2 1PZ, UK

EXPERIMENTS AND RESULTS

H13 Tool Steel

Specimens of H13 tool steel were machined in the form of standard ASTM compact tension specimens 25.4 mm (1 inch) thick. They were heat treated, such that the second temper temperature was varied between 600°C and 680°C in order to alter the final hardness. The actual hardnesses produced were 672, 593 and 369 Hv. Approximate hardness scale/tensile strength conversions are shown in Table 1. Fracture toughness, threshold stress intensity factor range and fatigue crack growth rate tests were then performed using well known standard test techniques (ASTM E399, E647).

The results obtained are summarised in Table 2 and Fig. 1.

The fracture surfaces were examined in a SEM. The transition from a fatigue to a rapid fracture surface, although clearly visible by eye, caused no noticeable change of micromechanism of fracture when seen at high magnification. For both types of surface, the mechanism appeared to be a mixture of microvoid coalescence (predominant) and cleavage. No fatigue striations could be found, although at a much larger scale beachmarks, caused by interruptions in the loading cycle, could be seen by eye as concentric markings on the fatigue surfaces.

SAE Bearing Steel

Test techniques. Several research groups are investigating rolling contact fatigue as a crack growth process, and the suggestion has been made that Mode II sliding growth might play a significant role in this process, e.g. Smith (3), Hearle and Johnson (4). In order to investigate this in a high hardness material, a specimen geometry capable of being loaded in Mode I (tension) and in Mode II was required. In addition the specimen was required to be as simple as possible in order to minimise the expense of machining such difficult material. A literature search revealed an ideal specimen and loading system, first used by Hua et al (5), see Fig. 2. This type of four point edge notched bending specimen can be loading in a variety of ways to achieve combinations of ΔK_I and ΔK_{II} values. For our particular experiments heat treatments produced steels in extreme hardness range 690 to 780 Hv. It was found impossible to sharpen the chevron V-notch by other than spark erosion. Both for toughness and crack growth tests some way was needed for initiating sharp cracks at these starter sites. Attempts at conventional four point bending produced either nothing or a fractured specimen! However, successful pre-cracking was achieved by inverting the specimen and loading to a sufficiently high ΔK (compressive) to cause yielding. Cracks then initiated and grew in the residual notch tensile stress field on the unloading part of the fatigue cycle. Subsequent cycling was performed using symmetrical loading

TABLE 1 - Approximate conversions between Rockwell and Vickers Hardness numbers and corresponding strength (N.B. Non-linear scales!)

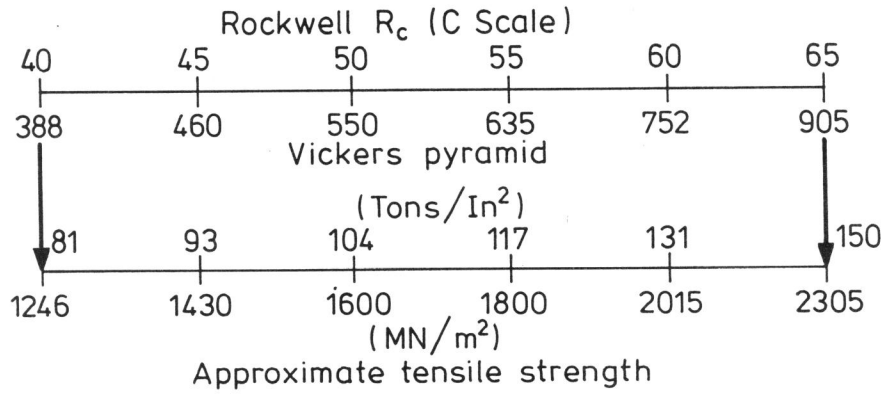

TABLE 2 - Hardness, threshold and fracture toughness results for H13 tool steel

Hardness (Hv)	Threshold, ΔK_{TH} R = 0.5 ($MNm^{-3/2}$)	Toughness, K_{IC} ($MNm^{-3/2}$)
672	4.5	35
593	-	70
369	6.3	75

to produce Mode I and asymmetrical loading to investigate Mode II growth. Again, standard testing, length measurement and data reduction techniques were used.

Bearing steel results. Mechanical properties data is listed in Table 3.

TABLE 3 - Yield, Hardness, threshold and fracture toughness data for SAE 52100 bearing steel

Hardness (Hv)	Yield (MNm^{-2})	Threshold, ΔK_{TH}	Toughness, K_{IC} ($MNm^{-3/2}$)
781	2200	No growth could be measured at $\Delta K < 6$ $MNm^{-3/2}$	12.8
738	-		-
721	1725		-
690	-		13.5

The growth rates, shown on Fig. 3, are pushed into a narrow band of ΔK values, between the threshold and toughness values. This squeezing effect is of course the reason why the production of crack growth rate data is so difficult.

Several tensile pre-cracked specimens were subjected to Mode II loading (see Fig. 2) for approximately 10^6 cycles at ΔK_{II} values between 2.5 and 10 $MNm^{-3/2}$. No Mode II crack growth could be detected, either by eye during the tests, or on subsequent sectioning. One pre-cracked specimen was loaded to failure in Mode II. Fracture occured at an angle of 70° to the existing crack direction, i.e. in a direction controlled by maximum tensile hoop stress generated by the Mode II loading.

Fractographic observations revealed a much greater proportion of cleavage fracture on the fatigue surface compared with the observations on the much softer H13 steel. No striations were observed and, again, there was little noticeable difference between the fatigue and rapid fracture surfaces.

DISCUSSION

Fatigue Crack Growth Rate Comparisons

The earliest results in the sparse literature for crack propagation in hard steels are those of Yokobori and Aizawa (6). They reported data for an unspecified high-hardened heat treatment ball bearing steel with measured hardness Hv 822. The results were obtained from a single test on a smooth specimen, where semi-circular or semi-elliptical cracks initiated from a non-metallic

inclusion near the specimen surface. Given their difficulties of crack measurement and data reduction, their results are satisfyingly close to our own obtained for similarly hardened 52100, see Fig. 4.

Averbach (7) reported data for a group of steels, (52100, M-50 and 18-4-1), obtained from compact tension specimens, hardened to the range Hv 752 - 905. Again the upper range of his data nearly coincides with our own for 52100. Our results for H13, whilst only slightly lower than those for the more hardened steels in the mid-range of growth rates, fall considerable lower than the hard steels over the range where growth rates are able to be sustained as the high fracture toughness is approached.

Also included in Fig. 4 is typical data for a structural (mild) steel, for which the threshold is similar to that observed for the hard steels, but once stable growth is achieved at rates higher than 5×10^{-6} mm/cycle, this soft material demonstrates a much slower growth rate than the hardened steels.

Simple models of crack propagation caused by crack tip stretching lead to dependence on growth rates inversely proportional to the yield stress. High strength materials demonstrate a trend in the opposite direction, e.g. the higher the hardness, the faster the growth rates, simply because the low toughness of high strength materials causes cleavage fracture modes to either superimpose upon or supersede ductile stretching, leading to much enhanced growth rates. The trend from structural steel, medium hardness H13 and high hardness steels is clear from Fig. 4.

Practical Implications

Stable crack growth has been observed in many contact fatigue situations. Because the stress fields are predominantly compressive. it is thought that reversed shear stresses are an important driving force for crack growth. Additionally Smith and Smith (3), have reported spherical debris formation in shear cracks; the same kind of spherical debris are a characteristic of bearing failures in rolling contact. However, our tests on a bearing steel failed to produce any Mode II crack growth. In a rolling contact situation where the crack surfaces are held in contact by compressive stresses it is probably even harder to promote sliding growth.Frictional resistance between opposing faces will probably lock the crack and prevent movement, (8). The nature of the driving force in Mode II therefore continues to remain a mystery. One possible solution is the existence of strong, and as yet unidentified, tensile residual stress acting normal to the observed crack directions. The Mode I growth rates we have observed for the high hardness bearing steel are so fast, that failure would follow almost immediately on crack initiation if the driving force was unimpeded Mode I. This is not supported by observation of crack development in ball bearings.

Acknowledgements

BICC Research and Engineering Ltd and SKF European Research Centre are thanked respectively for the supply of H13 and 52100 specimens. Drs M C Smith and C S Shin's work in performing the tests is gratefully acknowledged.

SYMBOLS USED

ΔK_I, ΔK_{II} Applied stress intensity factor range Mode I (tensile) ($MNm^{-3/2}$) Mode II (shear)

ΔK_{TH} Threshold stress intensity range ($MNm^{-3/2}$)

K_{IC} Plane strain fracture toughness ($MNm^{-3/2}$)

R Stress ratio (minimum load/maximum load)

Hv, Rc Vickers pyramid and Rockwell (C scale) hardness values.

REFERENCES

(1) Hudson, C M and Seward, S K, Int. J. Fracture, Vol. 14, 1978, pp. R151-R184

(2) Hudson, C M and Seward, S K, Int. J. Fracture, Vol. 20, 1982, pp. R57-R117

(3) Smith, M C and Smith, R A, Wear, Vol. 76, 1982, pp. 105-128

(4) Hearle, A D and Johnson, K L, J. Mech. Phys. Solids, Vol. 33, 1985, pp. 61-81

(5) Hua, G, Brown, M W and Miller, K J, Fatigue of Eng. Mats. and Struct., Vol. 5, 1982, pp. 1-17

(6) Yokobori, T and Aizawa, T, Report of the Research Institute on Stress and Fracture, Tohoku University, Sendai, Japan, Vol. 13, 1977, pp. 75-78

(7) Averbach, B L, In Advances in Fracture Research, Pergamon, Vol. 2, 1981, pp. 623-630

(8) Smith, M C and Smith, R A, to appear in the ASTM STP of 1984 Symposium on Fatigue (Dallas)

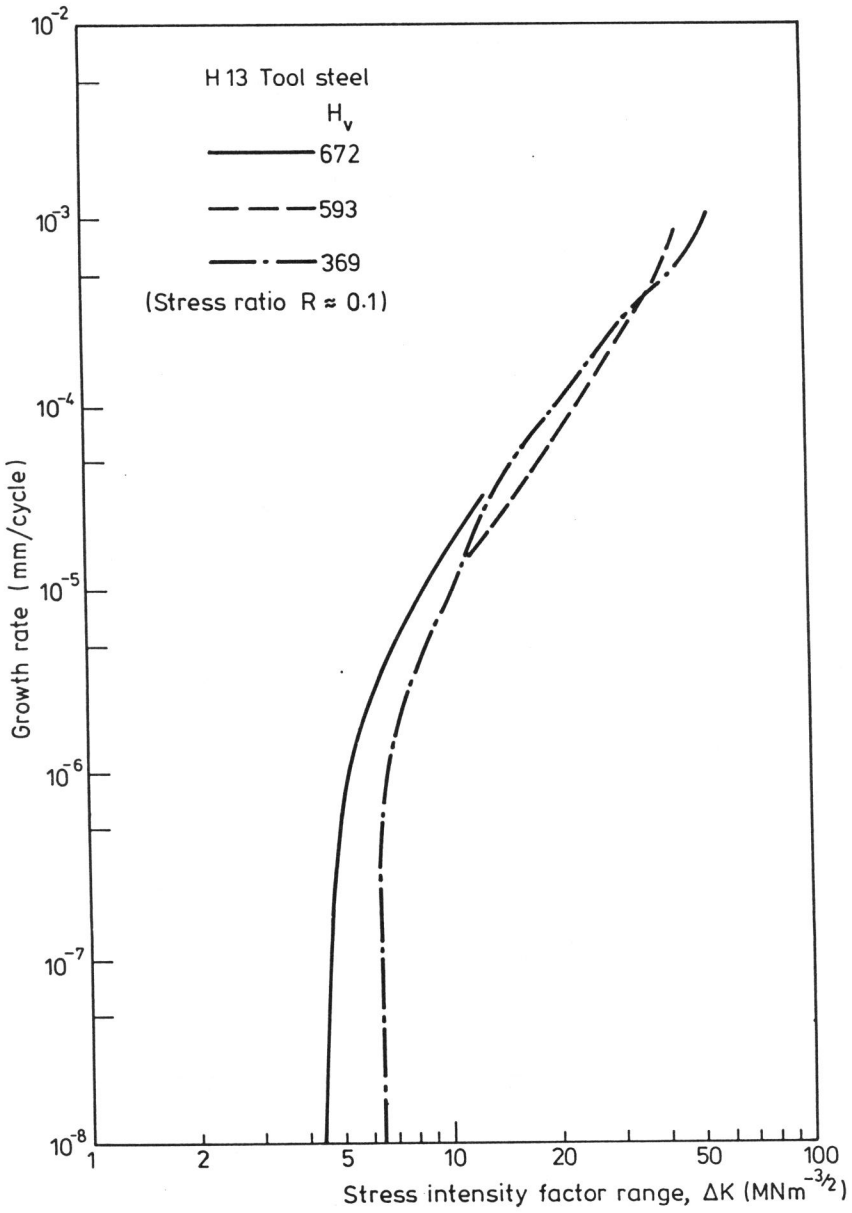

Fig. 1: Fatigue crack growth rates, H13

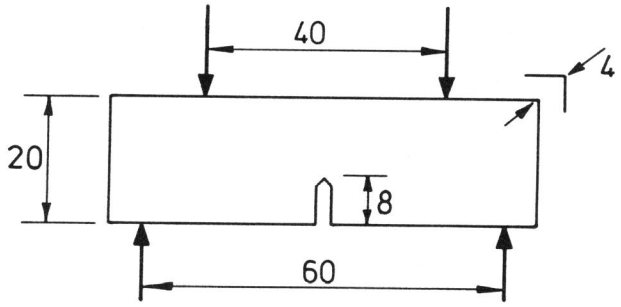

(a) 4 point bend specimen, tensile loading (dimensions in mm)

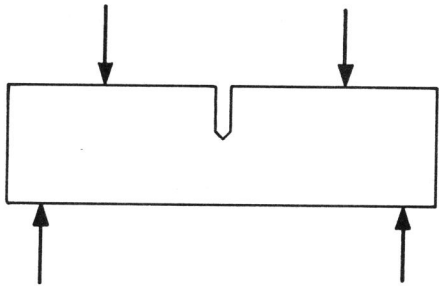

(b) Compressive crack initiation loading

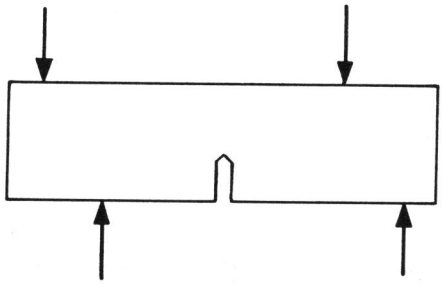

(c) Skew-symmetric Mode II loading (See Gua et al, Ref. 5)

Fig. 2: Chevron notched 4 point bending specimen showing various loading arrangements

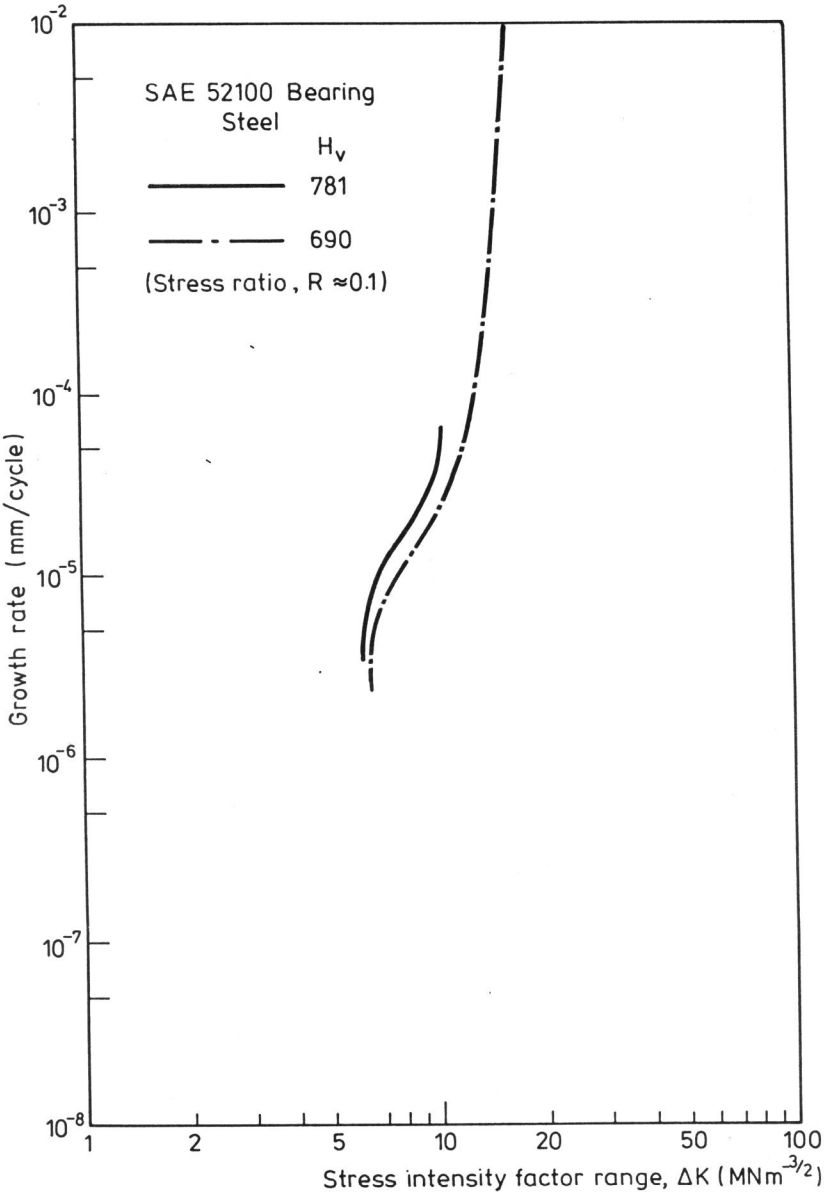

Fig. 3: Fatigue crack growth rates, SAE 52100

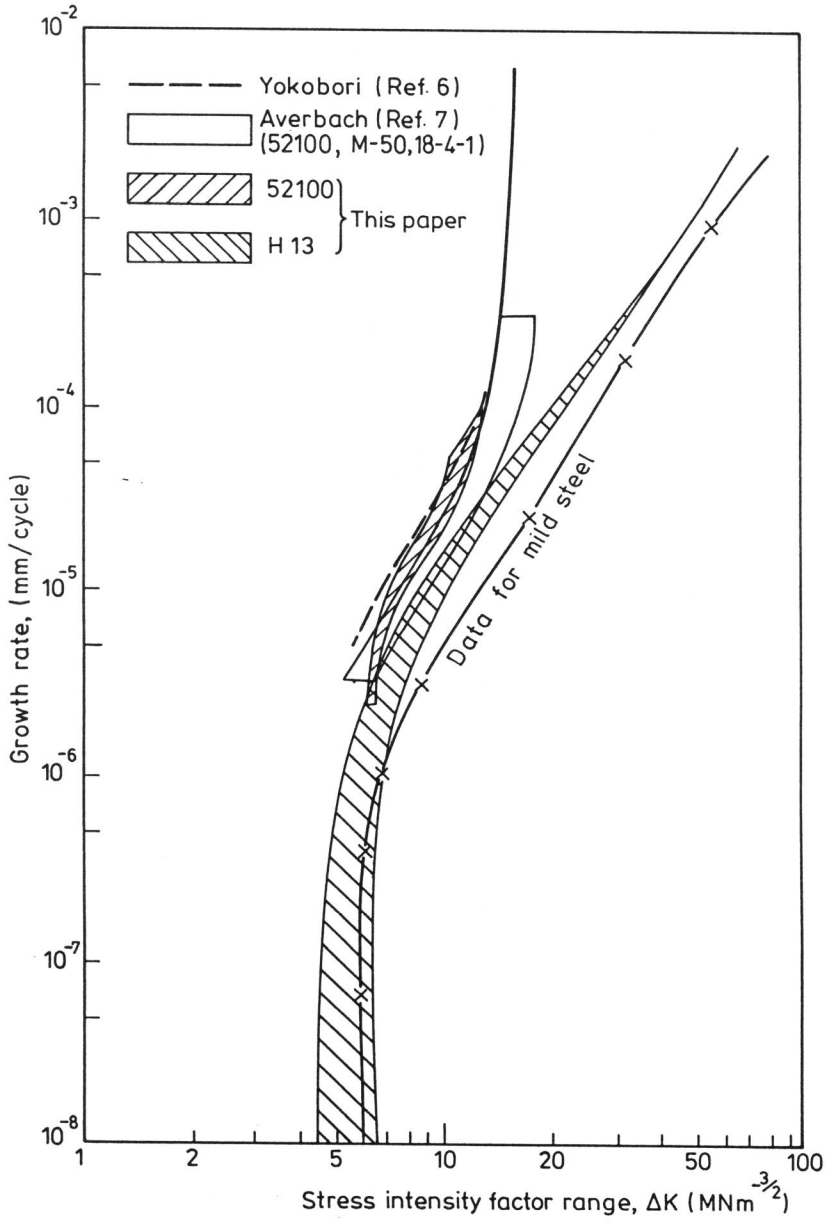

Fig. 4: Comparison of fatigue crack growth rates